Formation of Multinuclear Cells Induced by Dimethyl Sulfoxide: Inhibition of Cytokinesis and Occurrence of Novel Nuclear Division in *Dictyostelium* Cells

YOSHIO FUKUI

Department of Biology, Princeton University, Princeton, New Jersey 08544, and Department of Biology, Faculty of Science, Osaka University, Toyonaka, Osaka 560, Japan. Dr. Fukui's present address is Department of Biology, Faculty of Science, Osaka University, Toyonaka, Osaka 560, Japan.

ABSTRACT Our previous studies showed that 10% dimethyl sulfoxide (DMSO) induces the formation of actin microfilament bundles in the cell nucleus together with the dislocation of cortical microfilaments from the plasma membrane. The present study investigated the effects of DMSO on diverse activities mediated by cellular microfilaments as the second step toward assessing potential differences between nuclear and cytoplasmic actins of *Dictyostelium mucoroides*. DMSO was found to reversibly inhibit cell-to-glass as well as cell-to-cell adhesion, cell locomotion, and cell multiplication, whereas cytoplasmic streaming and phagocytosis were not obviously inhibited.

Also, 5% DMSO inhibited cytokinesis but did not totally inhibit cell growth thus leading to the development of giant cells more than 10 times larger than normal cells. Transmission electron microscopy using serial thin sections showed the occurrence of multinucleation in the DMSO-induced giant cells. After the removal of DMSO, the giant multinuclear cells underwent multiple cytoplasmic cleavage producing normal-sized mononuclear cells.

The nuclear division in the DMSO-induced giant cells was unique in that no spindle microtubules were formed, and vesicles appeared inside the nucleus forming a transverse partition of the nuclear envelope. The presence of actin filaments in those nuclei was demonstrated by a binding study with skeletal muscle myosin subfragment-1, and their possible involvement in this mode of nuclear division is discussed.

Since Ryser (30) first found microfilaments in the nuclei of *Physarum polycephalum*, considerable evidence showing the localization of actin in the cell nucleus has accumulated. Ultrastructural studies have proven the existence of actin filaments in mitotic cell nuclei of crane fly (3) and locust (17) testes. Actin has also been identified in nuclear as well as chromosome nonhistone proteins in rat liver (8), *P. polycephalum* (19), and *Dictyostelium discoideum* (22). We found that dimethyl sulfoxide (DMSO) induces the formation of huge microfilament bundles of actin in the *Dictyostelium* nucleus (13). We have shown that this formation of nuclear bundles could also be induced in interphase nuclei of *Amoeba proteus*, HeLa cells (14), and *Tetrahymena pyriformis* and Friend's leukemic cells of mouse (Katsumaru and Fukui, manuscript in preparation).

Forer and Jackson (12) and Forer (11) found actin filaments in *Haemanthus* endosperm, and proposed that the microfilaments play a role in chromosome separation during mitosis together with microtubules. Sanger and Sanger (31) and Cande et al. (6) also presented data showing the involvement of actin filaments in mitotic spindle bodies of rat kangaroo cells by fluorescein isothiocyanate-heavy meromyosin binding and indirect immunofluorescence technique, respectively. The organization and content of nuclear actin were discussed in relation to the growth state, as well as the malignant transformation of cells of mouse embryonic fibroblast (4) and Chinese hamster ovary cells (24). Rubin et al. (29) demonstrated that nuclear

THE JOURNAL OF CELL BIOLOGY · VOLUME 86 JULY 1980 181-189

actin is more highly polymerized than cytoplasmic actin in *A. proteus*, and that the nuclear actin might function in chromatin condensation.

The ultimate goal of our studies is to clarify the function of nuclear actin by verifying the mechanisms of microfilament organization in vivo and the potential differences between nuclear and cytoplasmic actins. To reach this goal, we have examined the dynamic formation and reversion of nuclear actin microfilaments and factors affecting their bundling (15). The present study is the next step: namely to examine how the properties of nuclear actin differ from those of cytoplasmic actin. In this respect, DMSO is a powerful tool for the study of microfilament organization, because a high concentration of it induces the formation of bundles of nuclear actin microfilaments (13, 14), and its effect on the cytoplasmic microfilaments is different thereby causing a dislocation of the filaments from the plasma membrane (15).

This study examined the effects of low concentrations of DMSO on diverse motile activities of cells in terms of adhesiveness, phagocytosis, cytoplasmic streaming, locomotion, and multiplication. DMSO reversibly inhibited some of these activities in *Dictyostelium mucoroides* cells. In addition, DMSO affected the growing cells by inhibiting cytokinesis. In such giant cells, a novel nuclear division occurred resulting in the formation of highly multinucleated cells. Furthermore, a binding study with rabbit skeletal muscle myosin subfragment-1 (S-1) verified the existence of actin microfilaments in those nuclei, which may be responsible for this mode of nuclear division.

MATERIALS AND METHODS

Cell Cultures

D. mucoroides, strain Dm-7, was cultured on nutrient agar plates with *Escherichia coli* (B/r) at 22°C (5). At the confluent stage, the cells were washed with Bonner's salt solution (10 mM NaCl, 10 mM KCl, 3 mM $CaCl_2$) by centrifugation (150 *g*, 2 min). For a liquid-shake culture, the method of Fukui and Takeuchi (16) was used: The cells were suspended in 1/60 M Na/K-Sörensen's phosphate buffer (pH 6.5) containing the bacteria and then incubated on a reciprocating shaker (110 rpm) or an 8-shaped shaker (50 rpm) at 22°C.

DMSO Treatment

The cells were washed with Bonner's salt solution and then resuspended in the salt solution containing various concentrations of DMSO.

Cell Adhesion Test

The cell-to-glass adhesion test was performed using the method of Yabuno (38). The cells at the early aggregation stage were washed three times with cold distilled water. The final pellet was suspended in Bonner's salt solution containing various concentrations of DMSO. A portion of the suspension was placed on an acid-washed glass coverslip and allowed to stand for 20 min. The coverslip was gently rinsed in the salt solution, and the number of the cells (n_o) fixed in a 0.04-mm^2 area was counted using an eyepiece grid micrometer (Sylvox Scientific Co., Morris Plains, N. J.) under a phase-contrast microscope. Next, the coverslip was washed with the salt solution (flow rate: 50 ml/30 s), and the number of remaining cells (n) was counted in the same field. The degree of adhesiveness was represented by the percentage of cells remaining ($n/n_o \times 100$).

The cell-to-cell adhesion test involved the suspension of cells in the salt solution containing 0 (control), 5, or 10% DMSO at a density of 10^7 cells/ml. The 10-ml suspension was placed in a 125-ml Erlenmeyer flask and incubated on a reciprocating shaker (110 rpm) at 22°C. The inhibition of adhesion by DMSO was estimated by counting the total number of particles (cells and aggregates) after 5, 15, 30, and 60 min of incubation.

Cell Locomotion Test

Cells at the early aggregation stage were washed three times with cold Bonner's salt solution, and the salt solution was added to the final pellet to make a suspension of 10^8 cells/ml. The cells were suspended in various concentrations of DMSO diluted with the salt solution to make a suspension of 10^7 cells/ml. After 15 min, a portion of the sample was placed on a slide glass covered with a thin layer of agar. The excess suspension was removed after 15 min and the sample was then covered with a thin glass slip. At least 40 cells in three different fields were observed under a phase-contrast microscope to trace their movement for 20 min. The trails of the cells were plotted on a section paper by using the eyepiece grid micrometer, and their locomotion distance was estimated using a map measure. The degree of cell locomotion was represented by the average velocity of the cells (micrometers per hour).

Measurement of Packed Cell Volume

Cells were separated from the remaining bacterial food supply by three successive low-speed centrifugations (150 *g*, 2 min). Afterwards the cells were sedimented in McNaught and Mackey-Shevsky-Stafford sedimentation tubes (Owens-Illinois Inc., Vineland, N. J.) by centrifugation (275 *g*, 3 min), and the packed cell volume was read directly from the scale of the tube.

Nuclear Number

A portion of the cell suspension was placed between a glass slide and a thin glass coverslip. Excess salt solution was removed with a piece of filter paper. After a while, the cells were squashed naturally by the surface-tension pressure, resulting in the extrusion of the nuclei. The nuclei could be identified by their size, dark nucleoli, and moderate light density of their matrix under a dark-contrast phase-contrast microscope. The extruded nuclei were counted while under the microscope.

S-1 Binding Study

Rabbit skeletal muscle myosin was purified according to the method of Perry (23). S-1 was separated from freshly prepared myosin according to the method of Weeds and Taylor (34). A single peak of the S-1 sample was used after the Sephadex G-200 column chromatography instead of DEAE chromatography.

The binding study of S-1 was performed according to the method originally developed by Ishikawa et al. (18) and was recently modified by Begg et al. (2). Cells were glycerinated through 5, 10, 25, and 50% glycerol in G-solution (50 mM KCl, 5 mM Na-EGTA, 2 mM dithiothreitol, 5 mM $MgCl_2$, 10 mM Tris-HCl, pH 7.2) for 20 min each at 0°C. After the preparations had been kept at 4°C for 15 h, glycerol was removed at 0°C through 50, 25, 10, and 5% glycerol in H-solution (50 mM KCl, 5 mM Na-EGTA, 10 mM Tris-HCl, pH 7.2). The glycerinated preparations were treated with S-1 in H-solution (2 mg/ml) for 12 h at 0°C and then washed with H-solution for 1 h at 0°C.

Electron Microscopy

Cells were sedimented by centrifugation (150 *g*, 2 min), and the pellet was embedded in 2% agar. Small pieces of agar (~1–2 mm^3) containing the cells were processed for electron microscopy using the method of Fukui (13). They were fixed with a mixture of 1% paraformaldehyde and 1.25% glutaraldehyde, postfixed with 1% OsO_4, and embedded in Spurr's resin. Just before the fixation of S-1-treated cells, the fixative was mixed with tannic acid to make a 0.5% solution in accordance with the method of Begg et al. (2). Thin sections (~1,500 Å thick) were prepared in an Ultrotome III (LKB Instruments, Inc., Rockville, Md.) with a diamond knife (DuPont Instruments, Wilmington, Del.). The sections were stained with 25% uranyl acetate in methanol and Reynolds' lead citrate, and were observed under a JEM 100-C electron microscope.

Chemicals Used

DMSO (Sigma Chemical Co., St. Louis, Mo.; Merck Chemical Div., Merck & Co., Inc., Rahway, N. J.), glutaraldehyde, paraformaldehyde, and Spurr's low viscosity embedding medium (Polysciences, Inc., Warrington, Pa.), osmium tetroxide (Merck Chemical Div.), and Sephadex G-200 (Pharmacia Fine Chemicals, Div. of Pharmacia Inc., Piscataway, N. J.) were used.

RESULTS

Effects of DMSO on Cell Adhesion

Adhesion of the cells to glass was inhibited by the treatment with DMSO (Fig. 1). The adhesiveness diminished in the inverted sigmoidal way as the concentration of DMSO increased from 1 to 10%. This inhibition of the adhesion disap-

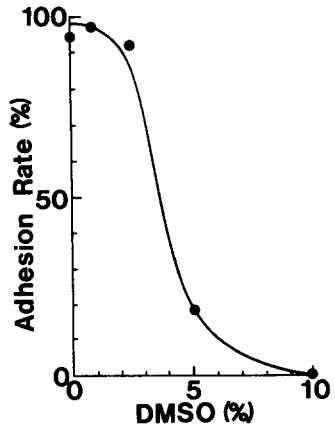

FIGURE 1 Reduction in cell-to-glass adhesiveness of *D. mucoroides* cells by DMSO. The adhesion rate is represented by the percent of cells remaining on the glass surface after washing with the flow of salt solution.

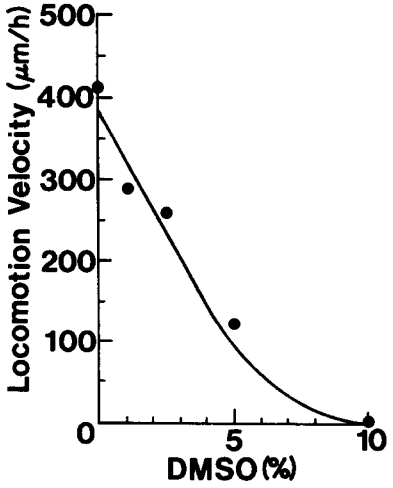

FIGURE 2 Inhibition of cell locomotion by DMSO in *D. mucoroides* cells. The locomotion rate is represented by the average velocity of the cells (micrometers per hour).

peared within 60 min after washing the cells with salt solution.

Cell-to-cell adhesion was also susceptible to DMSO. After a 15-min incubation, the total particle number of the cells in 0, 5, or 10% solution was 10, 31, or 42% of the initial cell number, respectively. This inhibition of the cell-to-cell adhesion remained almost constant during the following 30 min, and disappeared within 30 min after the washing.

Effects of DMSO on Cell Locomotion

The average locomotion velocity of the cells diminished with increasing concentrations of DMSO, and 10% DMSO totally inhibited the locomotion (Fig. 2). It was also apparent that the treatment with DMSO caused distinct changes in cell shape. In 0 or 2.5% DMSO, the cells formed many long filopodia on membrane ruffles at their anterior ends. In 5% DMSO, filopodium formation was totally inhibited, and under a phase-contrast microscope, only a single broad pseudopodium (lobopodium) at the anterior end was observed. In 10% DMSO, the cells were rounded-up and displayed no locomotion.

Effects of DMSO on Cell Growth

At 0–2.5%, DMSO had virtually no effect on cell multiplication. However, in 5% DMSO, the growth of the cells, estimated by cell number per milliliter, was inhibited. The doubling time of the cells incubated in 5% DMSO was 7.5 h on the average, whereas it was 3.0 h in 0, 1, or 2.5% DMSO. When the cultures were started at the cell density of 1×10^5 cells/ml, the final yield of the cells after a 48-h incubation was $\sim 5 \times 10^7$ cells/ml in 0–2.5% DMSO, whereas it was 5×10^6 cells/ml in 5% DMSO.

A dramatic difference was that the diameter of the cells incubated in 5% DMSO increased up to 11–12 μm (Fig. 3), whereas the diameter of the control cells was on the average 7–7.5 μm after a 48-h incubation. The packed volume of the cells incubated in 5% DMSO was 0.14 ml/10^8 cells, whereas it was 0.05 ml/10^8 cells for the control cells. This increase in cell size in 5% DMSO therefore must involve growth.

Effects of DMSO on Other Motile Activities

Active non-Brownian movement of granules was evident in the cytoplasm of cells treated with DMSO at concentrations as high as 10%. Series of serial thin sections of whole cells also demonstrated that many bacteria were engulfed by cells cultured in 5% DMSO through apparently normal phagocytosis. These results showed that cytoplasmic streaming and phagocytosis obviously were not inhibited by DMSO at concentrations that resulted in the rounding-up of cells as well as the inhibition of locomotion.

Multinucleation Induced by DMSO

Cells that had been cultivated in 5% DMSO had single large nuclei at their late growth stage when viewed with a phase-contrast microscope, whereas cells at their confluent stage had multiple normal-sized nuclei. The number of nuclei in those multinuclear cells was estimated using a phase-contrast microscope (Fig. 3 *b*); 92% was multinucleate and 9% (8 of the 92%) contained more than 10 nuclei, whereas in control cultures, only 1% was binucleate and 99% was mononucleate (Fig. 4).

The multinuclear cells resulting from 5% DMSO treatment underwent multiple cytoplasmic cleavage producing active normal cells after washing with the salt solution (Fig. 3 *c*). These washed cells were able to form normal fruiting bodies when they were incubated on agar plates. Interestingly, the diameter of the spores (5.5 ± 1.8 μm) was larger than that of the control spores (4.9 ± 0.8 μm); some of the spores were banana-shaped, making them unique to polyploid cells (16).

The ultrastructure of the giant cells that developed in 5% DMSO was investigated by transmission electron microscopy. Cells at the late growth stage contained single large nuclei that were ~10 μm in diameter (Fig. 5 *a*). Such large nuclei were round and contained peripheral nucleoli of high electron density. Interestingly, a portion of the nuclear envelope had a unique outpocketing structure, and this projection was associated with a possible microtubule-organizing center called a spindle pole body (20) or nuclear-associated body (NAB) (27, 28) (Figs. 5 *a* and 7 *a*). The high-magnification micrograph of this structure clearly showed that many microtubules originated from the electron-dense disk-shaped structure, confirming that this structure was identical to NAB (Fig. 5 *b*).

Cells at the confluent stage also contained multiple normal-sized nuclei that were ~3 μm in diameter. The multinuclear state of the cells was clearly demonstrated by serial thin sections of several cells: one of them is illustrated in a reconstituted mode from 72 serial thin sections (Fig. 6). These serial thin

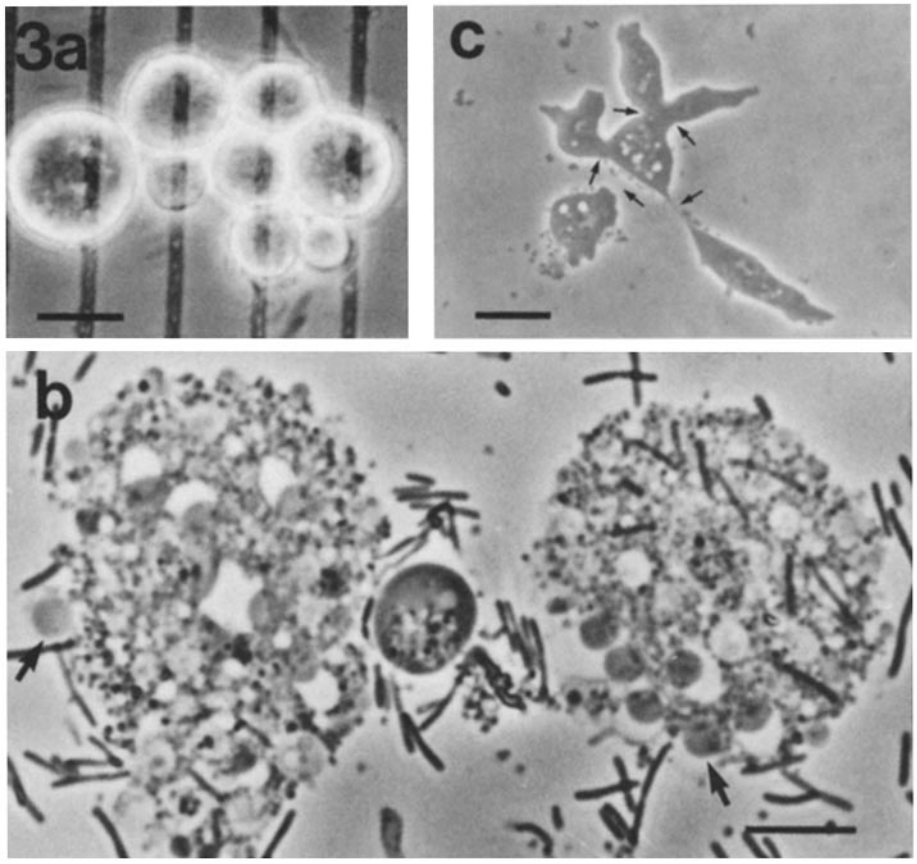

FIGURE 3 Phase-contrast microscopy of DMSO-induced giant multinuclear cells. (*a*) Cells grown in 5% DMSO for 48 h, showing the rounding-up of the shape and the variation in the size of the cells. × 1,150. (*b*) Squashed cells showing the extrusion of many nuclei. Nuclei could be identified according to their size, dark nucleoli, and moderate light density under a dark-contrast phase-contrast microscope. Two larger cells were squashed, but one smaller cell remained intact. Two typical nuclei are indicated by arrows. × 1,500. (*c*) A giant multinuclear cell performing cytoplasmic cleavage 1 h after the removal of DMSO. Cleavages are occurring at the points indicated by arrows. × 1,000. Bar, 10 μm.

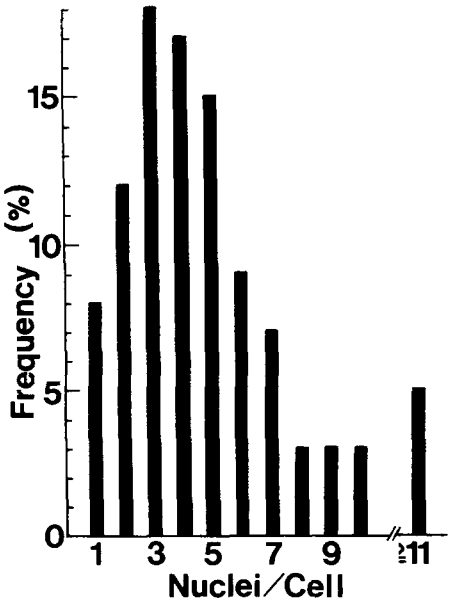

FIGURE 4 A histogram showing the frequency distribution of nuclei in cells incubated in 5% DMSO. An aliquot of cell suspension incubated for 48 h was put on a glass slide, and the nuclei were counted directly by the method described in the text. In controls, only 1% was binucleate, and the remaining 99% was mononucleate.

sections also showed that each nucleus was associated with a single NAB.

Novel Nuclear Division in DMSO-induced Giant Cells

During the late growth stage of cells, dumbbell-shaped nuclei were observed side by side with the large round nuclei. Serial thin sections showed that each portion of a dumbbell-shaped nucleus was associated with a single NAB. Inside these large or dumbbell-shaped nuclei, membranous structures forming clusters of vesicles were evident (Fig. 7*a*). The high-magnification micrograph of such nuclear vesicles showed that some portions of the vesicles were open to the nuclear matrix, suggesting that they may have been in the process of synthesis or membrane fusion (Fig. 7*b*).

In sections cut just beneath the nuclear envelope at the constricted region of the dumbbell-shaped nucleus, the nuclear vesicles were arranged like a transverse partition cutting the nucleus in two (Fig. 7*c*). It is noteworthy that the filamentous structure were observed running along the plane of constriction as if it was responsible for constricting the nucleus (Fig. 8*c*). The overall morphology of these filaments was ring-shaped, similar to the "contractile ring" of Schroeder (32). In sections of the central part of such dumbbell-shaped large nuclei or of normal-sized nuclei in multinuclear cells, a filamentous zone, ~160–180 nm thick, was evident along and beneath the inner

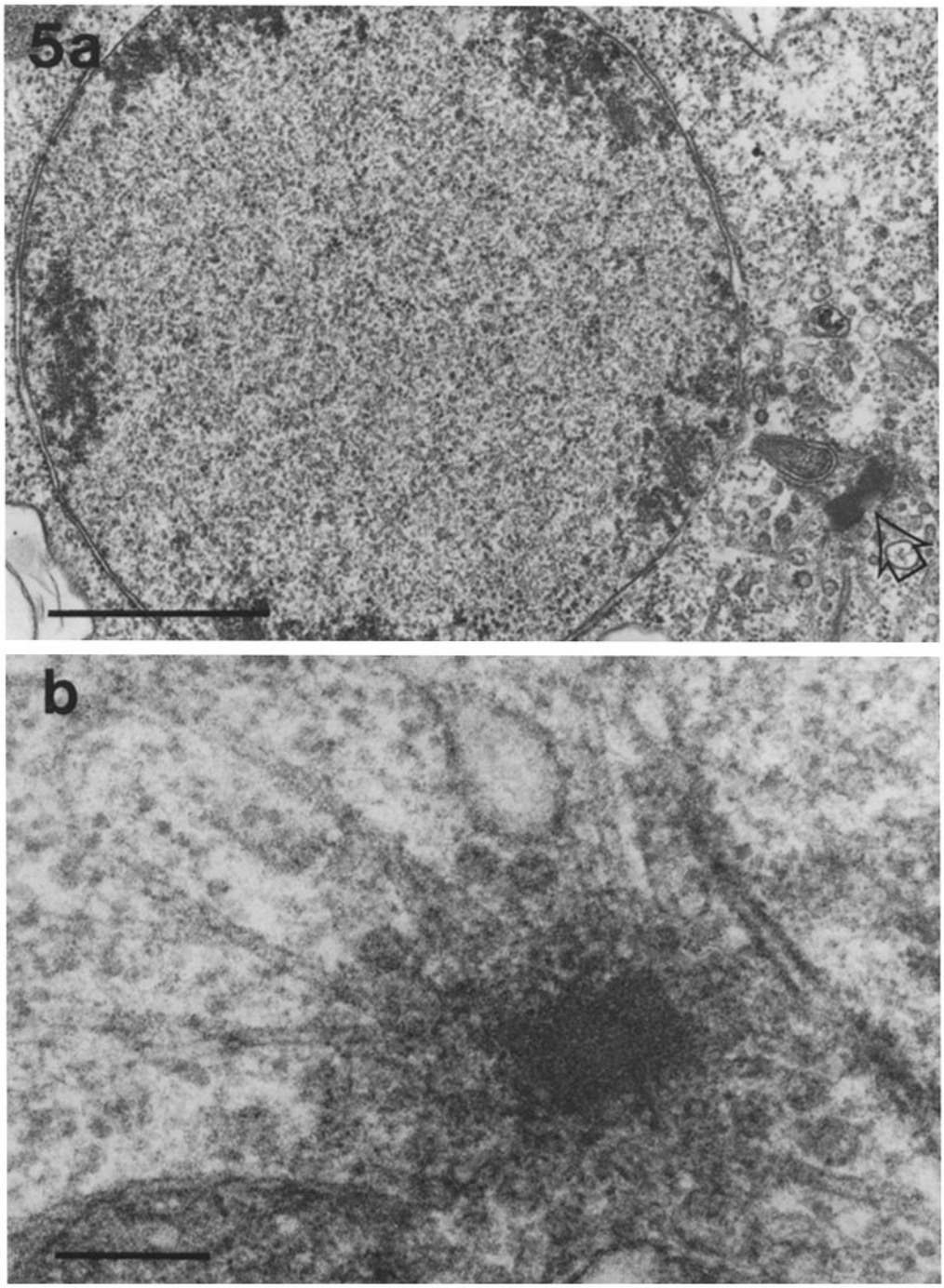

FIGURE 5 Transmission electron micrographs showing the fine structure of cells incubated in 5% DMSO. (*a*) A large round nucleus of a cell at the late growth stage that is associated with a NAB (arrow). An outpocketing of the nuclear envelope at the site of the NAB and cytoplasmic microtubules originating from the body are evident. The NAB looks like a doublet, suggesting that it has already finished the duplication which must precede nuclear division. × 32,000. Bar, 1 μm. (*b*) A high-magnification micrograph of a typical NAB showing the disk-shaped central body, vesicles in the surrounding matrix, and cytoplasmic microtubules originating from the complex. × 112,000. Bar, 0.2 μm.

membrane of the nuclear envelope (Fig. 8*a* and *b*). The diameter of each filament was 6.8 nm on the average according to examination of 25 cross sections of the filaments (Fig. 8*b*).

Once the DMSO-induced giant cells were glycerinated, the filamentous zone beneath the nuclear membrane could not be seen. However, a few microfilaments decorated with myosin S-1 were identified inside the nucleus of such giant cells. Interestingly, some of these actin filaments were present in the vicinity of the nuclear vesicles (Fig. 8*d*).

DISCUSSION

Effects of DMSO on Cell Adhesion and Locomotion

The present study shows that cell adhesion and locomotion of *D. mucoroides* cells are inhibited by DMSO. These inhibitions undoubtedly account for the effect of DMSO on aggregation during the development of the organism described in a

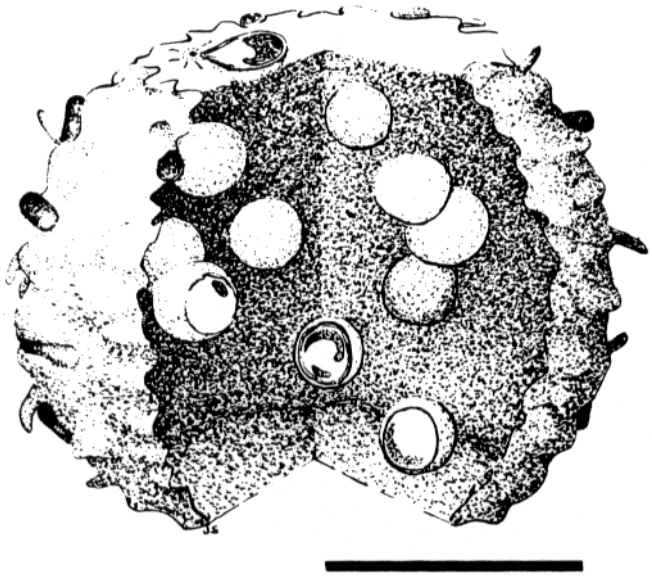

FIGURE 6 A three-dimensional drawing of a giant multinuclear cell reconstructed from 72 serial thin sections of a cell grown in 5% DMSO. This cell was at its confluent stage of the culture and contained 11 nuclei. Each nucleus was round and was associated with a single NAB. It is noteworthy that the formation of small spikes on the surface and the ability to engulf bacteria were not totally inhibited, although the overall morphology of the cell was round. Bar, 10 μm.

previous study (15). It is interesting that 5% DMSO also inhibits the formation of filopodia, which agrees with our previous finding that DMSO causes a dislocation of cortical microfilaments from the plasma membrane (15).

In other words, this dislocation may be the reason for the inhibition of filopodium formation, resulting in a reduction of the rate of locomotion. However, the cytoplasmic streaming, indicated by the active movement of granules, was not inhibited by DMSO, suggesting that DMSO might not act directly on the microfilament elements of the cellular contractile machinery, but rather may affect the interaction of the microfilaments with the plasma membrane.

Mechanism of Multinucleation and Its Physiological Meaning

Cytochalasin B inhibits cytokinesis resulting in the formation of multinuclear Earle's L cells (7) and human cultured lymphocytes (25). Cytochalasin B-induced multinuclear cells underwent "multiple cytoplasmic cleavage" after removal of the drug (7). Also, the mode of the increase in nuclear number is by "progressive addition" (25). These facts suggest that there are some similarities between the DMSO- and cytochalasin B-induced multinucleation. As I have indicated in the foregoing section, the inhibition of cytokinesis by DMSO might be through its action on the plasma membrane. This idea is attractive because it has also been suggested that cytochalasin B may also act on the plasma membrane by inhibiting "membrane fusion" during cytokinesis in Novikoff hepatoma cells (9).

Normal cells are less sensitive than virus-transformed cells in cytochalasin B-induced multinucleation, and only a small portion of the normal cells become multinucleate (1, 37). The DMSO-induced multinucleation in *D. mucoroides* resembled the case of transformed cells treated with cytochalasin B in that the frequency of the multinuclear cells was as high as 92% (Fig. 4).

The present study suggests that the inhibition of cytokinesis by DMSO initially caused the increase in nuclear and cellular volume (Figs. 5*a* and 7*a*). The large nucleus subsequently underwent a series of nuclear divisions producing multiple normal-sized nuclei in the cell. A DMSO-induced multinuclear cell, 13 times larger in volume than a normal cell, contained at least 11 nuclei. Obviously, a regulatory mechanism operated to keep the cytoplasm/nucleus ratio constant. This regulatory mechanism might be equivalent to that found during naturally occurring amitosis (26, 33, 36); it is probably a "means of increasing the nuclear surface and DNA content" (33).

Mechanism of the Unique Nuclear Division

After DMSO was removed, the large multinuclear cells underwent multiple cytoplasmic cleavage producing normal-sized mononuclear cells. However, large, banana-shaped spores were produced by some of these cells. This must indicate an increase in DNA content or polyploidization which occurred during the culture in 5% DMSO.

The novel nuclear division described in the present study is an alternative of normal mitosis. It is unique in that neither metaphase chromosomes nor spindle microtubules were observed, that no dispersion of nucleoli occurred, and that the nucleus was divided by a transverse partition of a newly organized nuclear envelope. This structure might be comparable to the "nuclear plate" named by Wilson (35) for the light-microscopic structure observed in animal cells performing amitosis. Each nucleus involved in the multinuclear cell was associated with a single NAB, and the nuclear envelope formed a prominent outpocketing in the vicinity of NAB (Figs. 5*a* and 7*a*). In interphase nuclei, NABs were linked to the nuclear envelope, and this connection remained intact after the nuclei were isolated by the method of Pederson (22) (our unpublished data). Furthermore, cytoplasmic microtubules originating from the NAB formed a radial cytoskeleton network as if they might anchor the nucleus. These observations suggest that the NAB complex, composed of nuclear envelope outpocketing, NAB, and microtubules, may determine the position of the nucleus and provide anchorage for the nucleus.

The change in the nuclear form to that of a dumbbell shape is probably related to the 160–180-nm-thick filamentous zone beneath the nuclear envelope, which is composed of 6.8-nm-thick filaments. This structure is apparently different from the nuclear lamina (reference 10, Fig. 20), or zonula nucleum limitans (21) in its morphology and dimensions (30 or 50 nm thick, respectively), but is rather similar to randomly oriented cytoplasmic microfilaments. Interestingly, the thickness of the filamentous zone matches that of the contractile rings in a variety of organisms (100–200 nm) (reference 32, p. 432), which have been established as being composed of actin. The present study demonstrates, by the binding study with myosin S-1, that actin filaments actually exist in dividing nuclei. Interestingly, some of these actin filaments could be identified in the vicinity of the nuclear vesicles, suggesting that they may function in organizing the nuclear vesicles to form the "nuclear plate," and at the same time, providing the force to constrict the nucleus to produce a dumbbell shape.

I express my sincere gratitude to Dr. John T. Bonner for his constructive criticisms during the course of this study and in the review of the manuscript. I am grateful for a grant from the Yamada Science

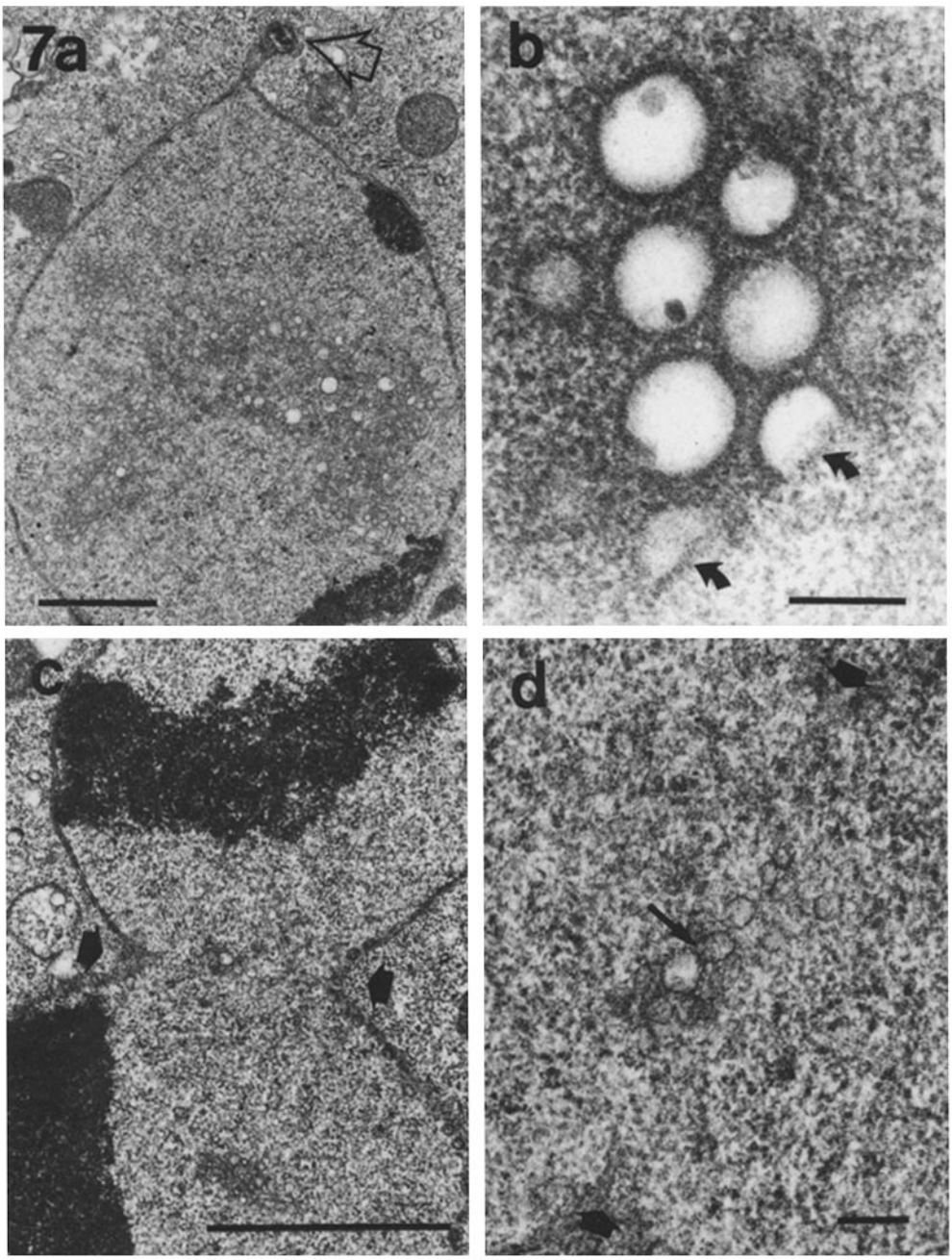

FIGURE 7 Transmission electron micrographs of cells incubated in 5% DMSO showing vesicular structure in the nuclei. (*a*) A large nucleus associated with an NAB (arrow) that was originating cytoplasmic microtubules. An outpocketing of the nuclear envelope at the point of the NAB and a vesicular structure inside the nucleus are apparent. This vesicular structure is probably a precursor of the nuclear envelope that will partition the nucleus in the nuclear division that follows. The electron-dense materials attached to the inner membrane are nucleoli. × 8,000. (*b*) A high-magnification electron micrograph of the nuclear vesicles. It should be noted that the vesicles are surrounded by electron-dense material, and that some portions of the vesicles are open to the nuclear matrix (arrows). × 80,000. (*c*) A dumbbell-shaped nucleus that is probably undergoing nuclear division. This section was cut just beneath the nuclear envelope at the constricted region of the nucleus, showing that the nuclear vesicles are arranged to form a transverse partition (nuclear plate; indicated by arrows). Oblique section of nuclear pore complexes are also apparent. × 17,000. (*d*) A high-magnification electron micrograph of the nuclear plate of (*c*). Some vesicles appear to be fusing to form a newly organized nuclear envelope (small arrow). × 48,000. (*a* and *c*) Bar, 2 μm. (*b* and *d*) Bar, 0.2 μm.

Foundation and for the hospitality of the Department of Biology, Princeton University for making it possible for me to perform the present study. I am indebted to Dr. James C. W. Chen for the discussion of amitosis, to Dr. George B. Witman for reviewing the manuscript, and to Joel Swanson for drawing a three-dimensional illustration of the multinuclear cell from the serial thin sections. My thanks are also given to Dr. Akio Inoue and Takayuki Miyanishi of the Department of Biology, Osaka University for the isolation of myosin S-1, and to Mrs. Hannah Suthers and Ms. Dorothy Spero for their help during the course of this study.

A part of this study was presented at the Cold Spring Harbor Meeting on Cell Motility, New York, 18 May 1979.

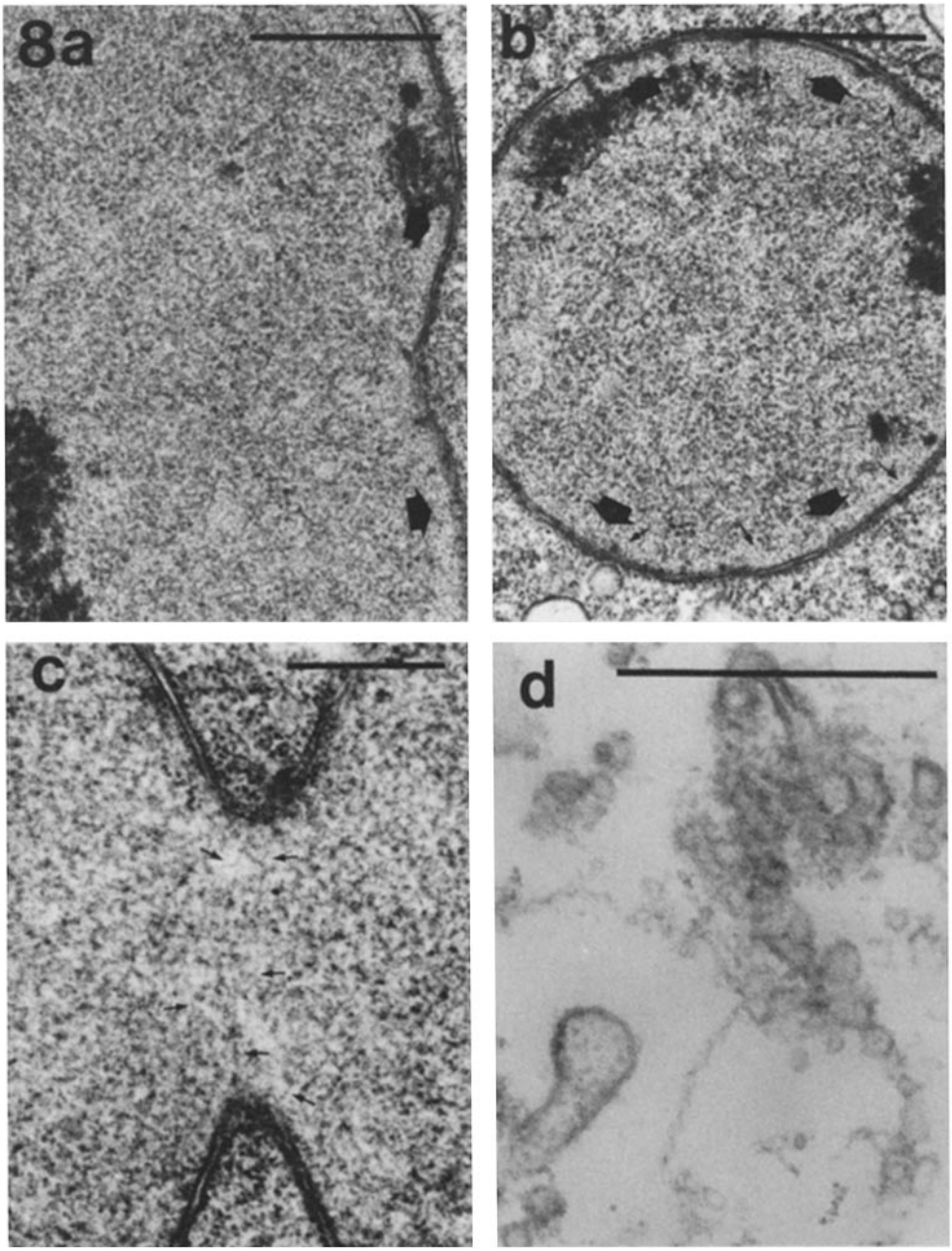

FIGURE 8 Transmission electron micrographs showing the nuclear microfilaments of cells cultured in 5% DMSO. (*a*) A longitudinal section of a large dumbbell-shaped nucleus. This section was cut at the center of the nucleus. A filamentous zone, ~160 nm thick, is evident beneath the nuclear envelope (arrows). × 26,000. (*b*) A relatively thick (~180 nm) thin section of a normal-sized nucleus in a multinuclear cell, showing the 180-nm-thick filamentous zone that is present beneath the nuclear envelope (large arrows). The diameter of the filaments estimated from 25 cross sections (small arrows) is 6.8 nm on the average. × 26,000. (*c*) A longitudinal section of a dumbbell-shaped nucleus, which was cut just beneath the nuclear envelope at the constricted region, demonstrating that thin filaments are oriented to form a ring structure surrounding the constricted region. × 43,000. (*d*) A high-magnification electron micrograph of a nuclear microfilament decorated with myosin S-1, confirming that this microfilament is actin. Note that the polarity of this filament is pointing to the nuclear vesicles, and that it finishes in the vicinity of the vesicles. × 88,000. (*a* and *b*) Bar, 1 μm. (*c* and *d*) Bar, 0.5 μm.

Received for publication 1 February 1980, and in revised form 18 March 1980.

REFERENCES

1. Altenberg, B. C., and S. Steiner. 1979. Cytochalasin B-induced multinucleation of murine sarcoma virus-transformed cells. Inhibition by sodium butyrate. *Exp. Cell Res.* 118:31–38.
2. Begg, D. A., R. Rodewald, and L. I. Rebhun. 1978. The visualization of actin filament polarity in thin sections. Evidence for the uniform polarity of membrane-associated filaments. *J. Cell Biol.* 79:846–852.
3. Behnke, O., A. Forer, and J. Emmerson. 1971. Actin in sperm tails and meiotic spindles. *Nature (Lond.).* 234:408–410.
4. Bertram, J. S., P. R. Libby, and W. M. Lestourgeon. 1977. Changes in nuclear actin levels with changes in growth state of C3H/10T 1/2 cells and the lack of response in malignantly transformed cells. *Cancer Res.* 37:4104–4111.
5. Bonner, J. T. 1947. Evidence for formation of cell aggregation by chemotaxis in the development of *Dictyostelium discoideum*. *J. Exp. Zool.* 106:1–26.
6. Cande, W. Z., G. Lazarides, and J. R. McIntosh. 1977. A comparison of the distribution of actin and tubulin in the mammalian mitotic spindle as seen by indirect immunofluorescence. *J. Cell Biol.* 72:552–567.
7. Carter, S. B. 1967. Effects of cytochalasins on mammalian cells. *Nature (Lond.).* 213:261–264.

8. Douvas, A. S., C. A. Harrington, and J. Bonner. 1975. Major nonhistone proteins of rat liver chromatin: Preliminary identification of myosin, actin, tubulin, and tropomyosin. *Proc. Natl. Acad. Sci. U. S. A.* 72:3902–3906.
9. Estensen, R. D. 1971. Cytochalasin B. I. Effect on cytokinesis of Novikoff hepatoma cells. *Proc. Soc. Exp. Biol. Med.* 136:1256–1260.
10. Fawcett, D. W. 1966. Nucleus. *In* An Atlas of Fine Structure: The Cell. Its Organelles and Inclusions. W. B. Saunders Company, Philadelphia. 2–48.
11. Forer, A. 1976. Actin filaments and birefringent spindle fibers during chromosome movements. *Cold Spring Harbor Conf. Cell Proliferation.* 3:1273–1293.
12. Forer, A., and W. T. Jackson. 1976. Actin in the endosperm spindles of the higher plant *Haemanthus katherinae* BAKER. *Cytobiologie.* 12:199–214.
13. Fukui, Y. 1978. Intranuclear actin bundles induced by dimethyl sulfoxide in interphase nucleus of *Dictyostelium. J. Cell Biol.* 76:146–157.
14. Fukui, Y., and H. Katsumaru. 1979. Nuclear actin bundles induced by dimethyl sulfoxide in *Amoeba proteus, Dictyostelium* and human HeLa cells. *Exp. Cell Res.* 120:451–455.
15. Fukui, Y., and H. Katsumaru. 1980. Dynamics of nuclear actin bundle induction by dimethyl sulfoxide and factors affecting its development. *J. Cell Biol.* 84:131–140.
16. Fukui, Y., and I. Takeuchi. 1971. Drug resistant mutants and appearance of heterozygotes in the cellular slime mould *Dictyostelium discoideum. J. Gen. Microbiol.* 67:307–317.
17. Gawadi, N. 1971. Actin in the mitotic spindle. *Nature (Lond.).* 234:410.
18. Ishikawa, H., R. Bishoff, and H. Holtzer. 1969. Formation of arrowhead complexes with heavy meromyosin in a variety of cell types. *J. Cell Biol.* 43:312–328.
19. Lestourgeon, W. M., A. Forer, Y. Yang, J. S. Bertram, and H. P. Rusch. 1975. Major components of nuclear and chromosome non-histone proteins. *Biochim. Biophys. Acta.* 379:529–552.
20. Moens, P. B. 1976. Spindle and kinetochore morphology of *Dictyostelium discoideum. J. Cell Biol.* 68:113–122.
21. Patrizi, G., and M. Poger. 1967. The ultrastructure of the nuclear periphery. The zonula nucleum limitans. *J. Ultrastruct. Res.* 17:127–136.
22. Pederson, T. 1977. Isolation and characterization of chromatin from the cellular slime mold, *Dictyostelium discoideum. Biochemistry.* 16:2771–2777.
23. Perry, S. V. 1952. Myosin adenosinetriphosphatase. *Methods Enzymol.* 2:582–588.
24. Puck, T. T. 1977. Cyclic AMP, the microtubule-microfilament system, and cancer. *Proc. Natl. Acad. Sci. U. S. A.* 74:4491–4495.
25. Ridler, M. A. C., and G. F. Smith. 1968. The response of human cultured lymphocytes to cytochalasin B. *J. Cell Sci.* 3:595–602.
26. Roberts, G., and J. C. W. Chen. 1975. Chromosome analysis and amitotic nuclear division in *Nitella axillaris. Cytologia (Tokyo).* 40:151–156.
27. Roos, U-P. 1975. Mitosis in the cellular slime mold *Polysphondylium violaceum. J. Cell Biol.* 64:480–491.
28. Roos, U-P. 1975. Fine structure of an organelle associated with the nucleus and cytoplasmic microtubules in the cellular slime mould *Polysphondylium violaceum. J. Cell Sci.* 18:315–326.
29. Rubin, R. W., L. Goldstein, and C. Ko. 1978. Differences between nucleus and cytoplasm in the degree of actin polymerization. *J. Cell Biol.* 77:698–701.
30. Ryser, U. 1970. Die Ultrastruktur der Mitosekerne in den Plasmodien von *Physarum polycephalum. Z. Zellforsch. Mikrosk. Anat.* 110:108–130.
31. Sanger, J. W., and J. M. Sanger. 1976. Actin localization during cell division. *Cold Spring Harbor Conf. Cell Proliferation.* 3:1295–1316.
32. Schroeder, T. E. 1973. Actin in dividing cells: Contractile ring filaments bind heavy meromyosin. *Proc. Natl. Acad. Sci. U. S. A.* 70:1688–1692.
33. Shen, E. 1967. Microspectrophotometric analysis of nuclear DNA in *Chara zeylanica. J. Cell Biol.* 35:377–384.
34. Weeds, A. G., and R. S. Taylor. 1975. Separation of subfragment-1 isoenzymes from rabbit skeletal muscle myosin. *Nature (Lond.).* 257:54–56.
35. Wilson, E. B. 1947. Cell division. VI. Direct Division. Fragmentation. Amitosis. *In* The Cell in Development and Heredity. 3rd edition. Macmillan Inc., New York. 214–223.
36. Wolfe, J. 1967. Structural aspects of amitosis: a light and electron microscopic study of the isolated macronuclei of *Paramecium aurelia* and *Tetrahymena pyriformis. Chromosoma (Berl.)* 23:59–79.
37. Wright, W. E., and L. Hayflick. 1972. Formation of anucleate and multinucleate cells in normal and SV_{40} transformed WI-38 by cytochalasin B. *Exp. Cell Res.* 74:187–194.
38. Yabuno, K. 1971. Changes in cellular adhesiveness during the development of the slime mold *Dictyostelium discoideum. Dev. Growth Differ.* 13:181–190.